17th World Conference on Earthquake Engineering, 17WCEE
Sendai, Japan - September 13th to 18th 2020

DETAILED EVALUATION OF YIELD DISPLACEMENT OF REINFORCED CONCRETE COLUMN

T. Asai[(1)], M. Teshigawara[(2)]

[(1)] *Assistant Professor, Nagoya University, asai.tatsuya@k.mbox.nagoya-u.ac.jp*
[(2)] *Professor, Nagoya University, teshi@corot.nuac.nagoya-u.ac.jp*

Abstract

Highly accurate evaluation of lateral load - displacement (Q - δ) relationship of a building is important to appropriately understand the seismic capacity of the building. Yield displacement in the Q - δ relationship is especially one of the key parameters which determine the seismic response of the building. It is also directly utilized in defining the damping factor in the calculation of response and limit strength [1] of a reinforced concrete building. Although the current evaluation methods of the yield displacement of a reinforced concrete member easily give an output, it can have an error that is not negligible[2]~[6]. We are, therefore, engaged in the researches to propose a highly accurate evaluation method of yield displacement of a reinforced concrete building. In this paper, we present a part of the research outcome obtained based on the static loading test of a reinforced concrete column specimen.

Firstly, we describe the outline of a loading test of a half-scale column specimen. In the loading test, we obtained detail displacement distribution of the specimen using the motion capture system to accurately obtain the flexural displacement and the shear displacement. Based on the motion capture data, rotation angle of the tension side concrete is found smaller than that of the compression side concrete because cantilever portion between two flexural cracks is pulled down by the downward force due to the flexural rebars. Displacement of only compression side is, therefore, considered in the discussion of the horizontal displacement of the column specimen as a component of a structural frame.

Secondly, flexural displacement is computed by integrating rotation angle of the compression side and compared with the calculated result based on the sectional analyses. The calculation is then found to underestimate the test results about 30 % at 1/200 rad. If it is modified considering the larger curvature at the bottom section observed in the loading test, the test results can be evaluated well. The reason of the larger curvature in the compression side of the test results is assumed that the stub (footing or beam in the actual structures) restrain the compression side concrete to increase the shear stress, accordingly, increase the curvature.

Thirdly, shear displacement is obtained by subtracting flexural displacement from the total displacement. It is then compared with the calculation results of the elastic shear displacement considering sectional area that excludes area of flexural crack and compression failure. They are found to be well correspond to each other.

Keywords: reinforced concrete; column; yield displacement; flexural displacement; shear displacement

1. Introduction

Highly accurate evaluation of lateral load - displacement (Q - δ) relationship of a building is important to appropriately understand the seismic capacity of the building. Yield displacement in the Q - δ relationship is especially one of the key parameters which determine the seismic response of the building. It is also directly utilized in defining the damping factor in the calculation of response and limit strength [1] of a reinforced concrete building. Although the current evaluation methods of the yield displacement of a reinforced concrete member easily give an output, it can have an error that is not negligible [2]~[6].

We are, therefore, engaged in the researches to propose a detailed method which evaluate yield displacement of a reinforced concrete building with high accuracy [7], [8]. In this paper, we present a part of the research outcome obtained based on the static loading tests of a reinforced concrete column specimen. Flexural displacement component and shear displacement component are obtained with high accuracy based on the displacement distribution obtained by motion capture. Their evaluation method is then investigated herein (the anchorage displacement is not focused in this paper).

2. Outline of loading test

2.1 Specimen and loading system

Cross section of the specimen, loading system, design parameters, and material properties are shown in Fig.1, Fig.2, Table 1, and Table 2, respectively.

Table 1 Specimen parameters

Aspect ratio	Axial load ratio	Shear span ratio	Flexural reinforcement	Shear reinforcement
2.0	0.25 %	2.6	5.72 %	2.40 %

Table 2 Material properties

Concrete			Rebar
Compression	Tensile	Youngs modulus	Tensile
27.6 N/mm^2	2.3 N/mm^2	22.6 kN/mm^2	393 N/mm^2 (D16), 360 N/mm^2 (D10)

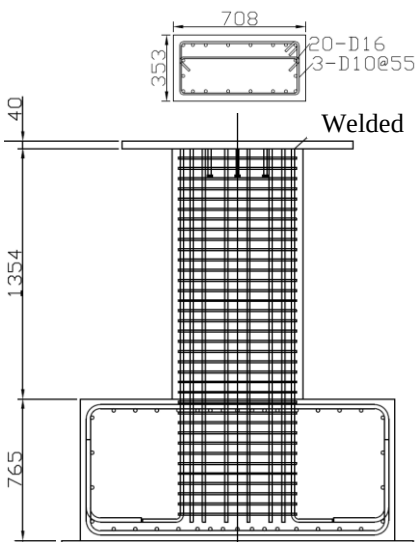

Fig. 1 Sectional view of specimen

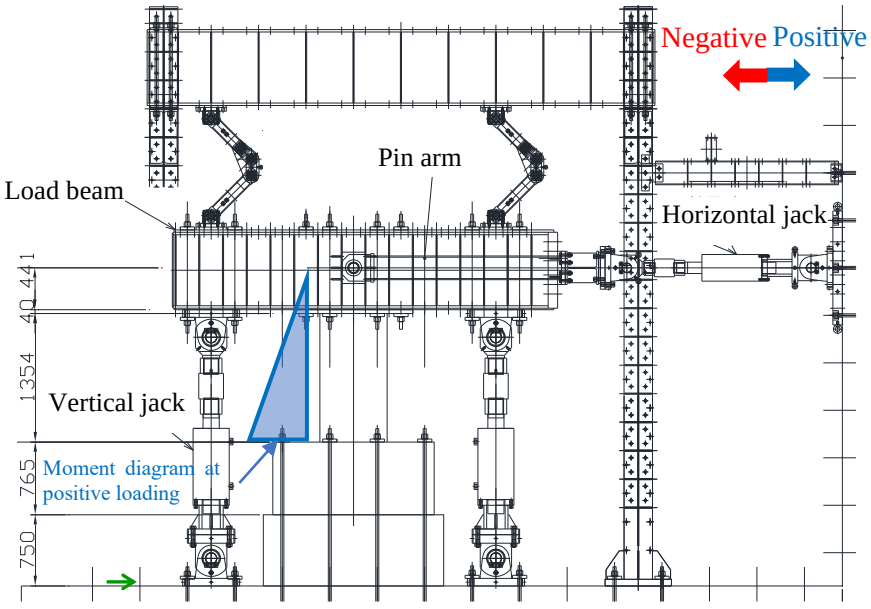

Fig. 2 Loading system

unit : mm

A 1st story column of a 6-story building is scaled down by half to determine the dimension of the specimen. Out of total height to the inflection point of the specimen (1835 mm), the RC part is 1354 mm. Remained part consists of half of load beam depth (441 mm) and steel plate thickness (40 mm). The center of the load beam is connected with pin joint to the horizontal oil jack. Axial load is applied to the specimen by two horizontal oil jack through the load beam. Loading is firstly controlled by the horizontal peak load of ±50 kN, ±100 kN, ±150 kN, and secondly controlled by the horizontal peak drift of ±1/800 (2), ±1/400 (2), ±1/200 (2), ±1/133 (2), ±1/100 (2), ±1/75 (2), ±1/50 (2) , +1/25 (1) rad. (inside the blackets show the number of the repeated cycle).

2.2 Horizontal load – horizontal displacement relationship

Figure 3 show the horizontal load - horizontal displacement relationship (Q-δ) obtained from the loading test. In the figure, red solid line and read dashed line show the simplified estimation following the current design method[2), 3)],which is empirically proposed based on the enormous number of loading test results, and horizontal capacity obtained based the sectional analyses assuming the plane section remains plan, respectively. At around 1/200 rad., compression side concrete reached its compression strength and a compression side rebar reached yield strength. At around 1/150 rad., tension side rebar started to yield. The estimated yield drift of 1/120 rad. [2), 3)] is larger than the test result.

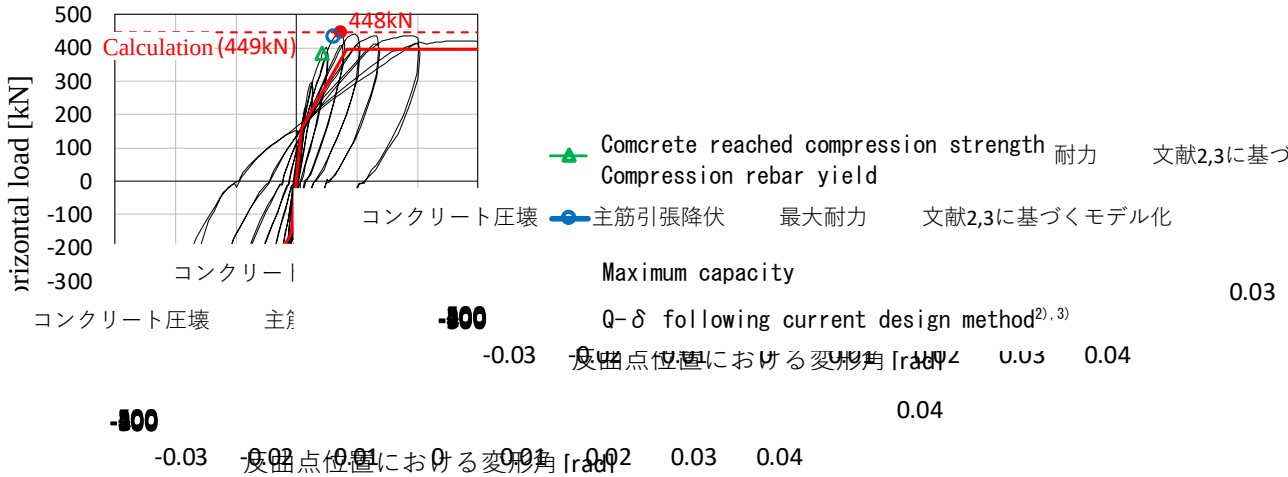

2.3 Detailed measurement of displacement distribution

To measure the detailed displacement distribution of the specimen, we installed motion capture system. In this system, the infrared cameras track 3-dimenstional locations of the reflection markers. We used three infrared cameras (Prime 41) and 177 markers of 12.7 mm diameter, both are produced by OptiTrackm, in the test. The original location of the markers is shown in Fig. 4 later: three markers are attached on the stub as the reference points, and the others are attached to the side surface of the specimen. Sampling rate is 100 Hz.

Before investigating the data, high frequency noise is filtered by taking average of continuous one hundred data (i.e., data during one second), and spike noise is eliminated and complimented with average value of two data of one step before and after. Data example of both before and after the filtering are shown in Fig.4.

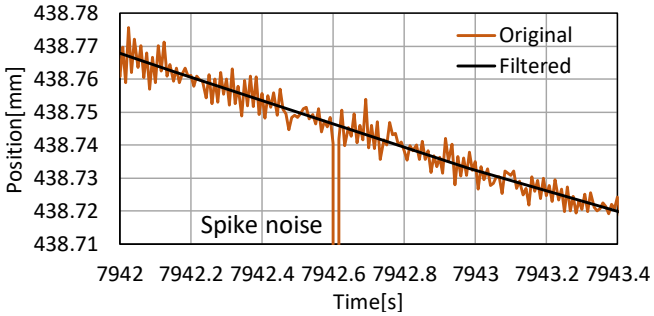

Fig. 4 Example of data filtering

3 Evaluation of displacement component based on detailed measurement

3.1 Displacement characteristics of specimen

Based on the data obtained above, displacement characteristics of the specimen is firstly investigated herein. Fig. 5 shows the displacement distribution and the crack drawing at the drift of 1/200 rad. Note that the surface of crack drawing and motion capture measurement are different. Displacement from the original location is multiplied by 100. In Fig. 5(a), sections between two major cracks (i.e., wider cracks) are surrounded by dashed line. Location of diagonal cracks which extent from those major cracks are indicated by ▽.

The figure shows the plane sections just above the major cracks remain plan. On the other hand, the plane sections just below those cracks does not remain plane: rotation angle of the tension side is lower than that of compression side. This result can clearly be observed by Fig. 6. Though the rotation angle of the compression side continuously increases, that of tension side steeply increase at the location of the crack. The diagonal crack is caused by the deformation difference between compression side and tension side.

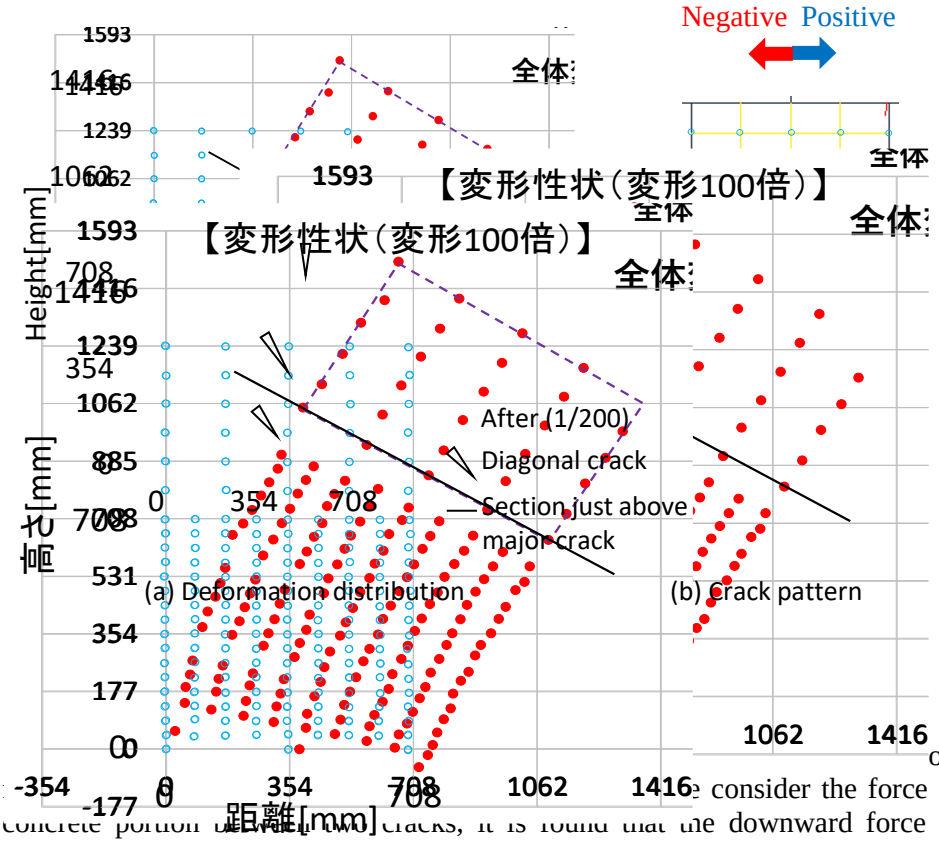

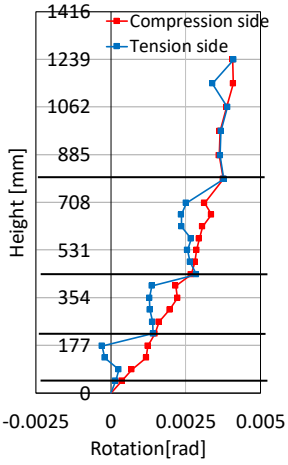

Fig.6 Rotation distribution at 1/200 rad.

o be caused by the downward e consider the force equilibrium on the cantilever concrete portion between two cracks, it is found that the downward force of rebars are excited by the differences of the rebar stress between above and below concrete portion. The moment is caused at the end part of the cantilever, which cause tensile stress. If we calculate that tensile stress σ_t of the column specimen by Eq. (1) at the timing of the occurrence of the second diagonal crack from the bottom, for example, it reaches 3.8 N/mm^2, which is larger than the tensile capacity of the concrete (2.3 N/mm^2 as shown in Table 2).

$$\sigma_t = M/Z = \Delta T\, d_{ns} /(B\, d_{ns}^2 /6) \quad (1)$$

where ΔT [kN] is the downward force on the cantilever excited by the rebars, d_{ns} [mm] is the horizontal distance between rebars and end part of the cantilever, B [mm] is the width of the specimen.

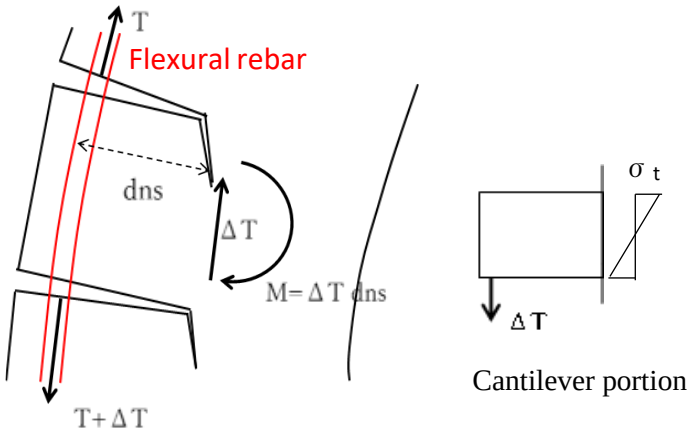

Fig. 7 Force equilibrium on the cantilever concrete portion between two flexural cracks

Considering the displacement characteristics mentioned above, we do focus on the displacement of the compression side in the next two sections to discuss the horizontal displacement of the specimen as a structural component of a frame.

3.2 Flexural displacement

Flexural displacement can be obtained by integrating rotation angle of the specimen, rotation angle of the compression side is used as was mentioned in the previous se e

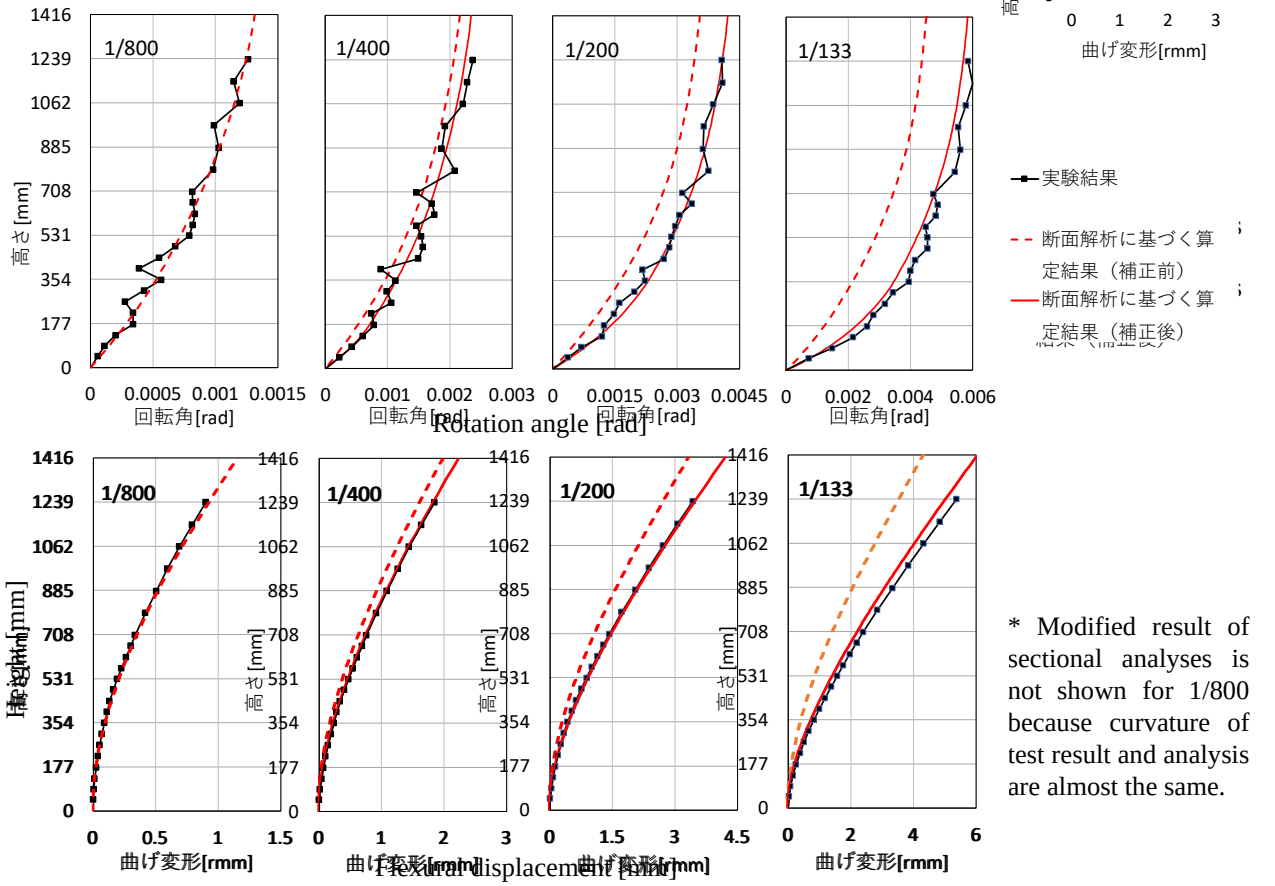

* Modified result of sectional analyses is not shown for 1/800 because curvature of test result and analysis are almost the same.

Fig. 8 Rotation distribution and flexural displacement distribution along specimen's height

distribution of the rotation angle and the flexural displacement along specimen's height at the peak of 1/800, 1/400, 1/200, and 1/133 rad. In the sectional analyses (red dashed line), the same moment distribution with the loading test is considered. The modified results of the sectional analyses results (it will be described later) are shown by the red solid line. As shown in the figure, the calculated result corresponds well to the loading test at 1/800 rad. After 1/400 rad., however, the calculations underestimate the test results: the flexural displacement of the calculation is, for example, 30 % smaller than that of the test result at 1/200 rad.

To investigate the difference of the rotation angle between the loading test and the calculation, rebar strain distribution at the bottom section of the specimen is shown in Fig.9, considering the difference of the rotation angle is caused by the difference of the curvature (i.e., strain distribution). As shown in the figure, results of the loading test and calculation corresponds well to each other at 1/800 rad. After 1/400 rad., however, the gradient of the strain (i.e., curvature) of the compression side becomes larger than the calculation. If we modify the calculation up to the height where difference between test results and calculations are observed (up to 180 mm height for 1/400 rad., and up to 350 mm height for 1/200 and 1/133 rad.) considering the curvature of the test results, the rotation angle and the flexural displacement of the test results can be evaluated very well (compare black line and red solid line in Fig. 8).

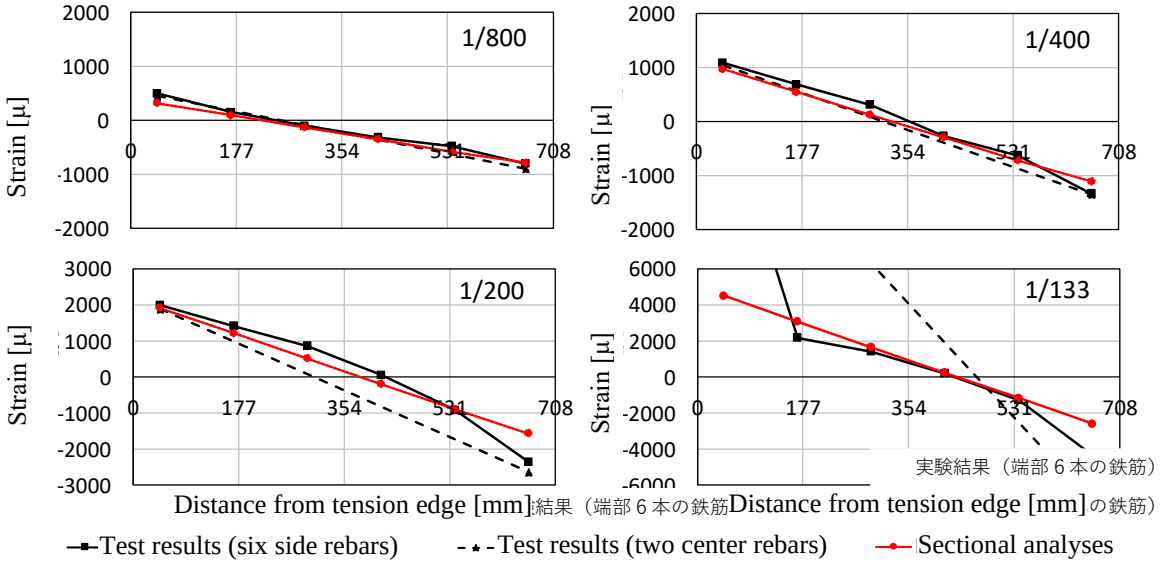

T reason ompression side at the bottom section is larger ir ess distr fects the flexural strain distribution, of the horizon Shear stress distribution is calculated using the following procedures. If we put x axis and z axis for the specimen's width direction and height direction, respectively, shear stress gradient to the x direction $d\tau_c/dx$ corresponds to the axial stress gradient to the z direction $d\sigma_c/dz$ as shown in Eq. (2).

$$\frac{d\tau_c}{dx} = \frac{d\sigma_c}{dz} \tag{2}$$

Shear stress is, therefore, expressed by Eq. (3).

$$\tau_c = \int \frac{d\tau_c}{dx} dx = \int \frac{d\sigma_c(\varepsilon_c)}{dz} dx \tag{3}$$

If we consider the following assumptions 1) to 3), shear stress τ_c can be computed using the measured strain values of flexural rebars ε_s (= concrete strain ε_c) at the different height.

1) Strain of flexural rebar ε_s and concrete ε_c at the same location is same.
2) Relationship between σ_c and ε_c of the cover concrete follows the concrete cylinder compression tests.
3) Core concrete is elastic with the stiffness of Young's modulus shown in Table 2.

As the strain values of the flexural rebars at the height of 0 D, 0.5 D, and 1.0 D (D is the depth of the specimen) are measured in the loading test, they are used for ε_c (= ε_s) to obtain σ_c in Eq. (3) (i.e., average shear stress between 0 D and 0.5 D, and 0.5 D and 1.0 D are computed).

Figure 10 shows the shear stress distribution along specimen's depth at 1/800, 1/400, and 1/200 rad. The result of 1/133 rad. are not shown in the figure because flexural rebar strain greatly exceeds the yield strain, and accordingly assumption (1) above is not applicable. In the figure, results based on the sectional analyses are also shown by read line. Dashed line and green solid line show the neutral axis location and average shear stress (shear force divided by specimen's horizontal sectional area). Shear stress of the cover concrete between 0 D – 0.5 D at 1/200 rad. is assumed zero because compression failure of the cover concrete was observed.

From the figure, shear distribution of the test results and that obtained based on the sectional analyses correspond to each other for 0.5 D – 1.0D. On the contrary, for 0 D – 0.5 D, difference between those two increases as the displacement increases: shear stress of the compression side computed based on the test result is larger than that calculated based on the sectional analyses. This difference is assumed to be caused by the restraint effect by the stub (footing or beam in the actual structures). It is important to quantify this effect for the highly accurate estimation of the flexural displacement.

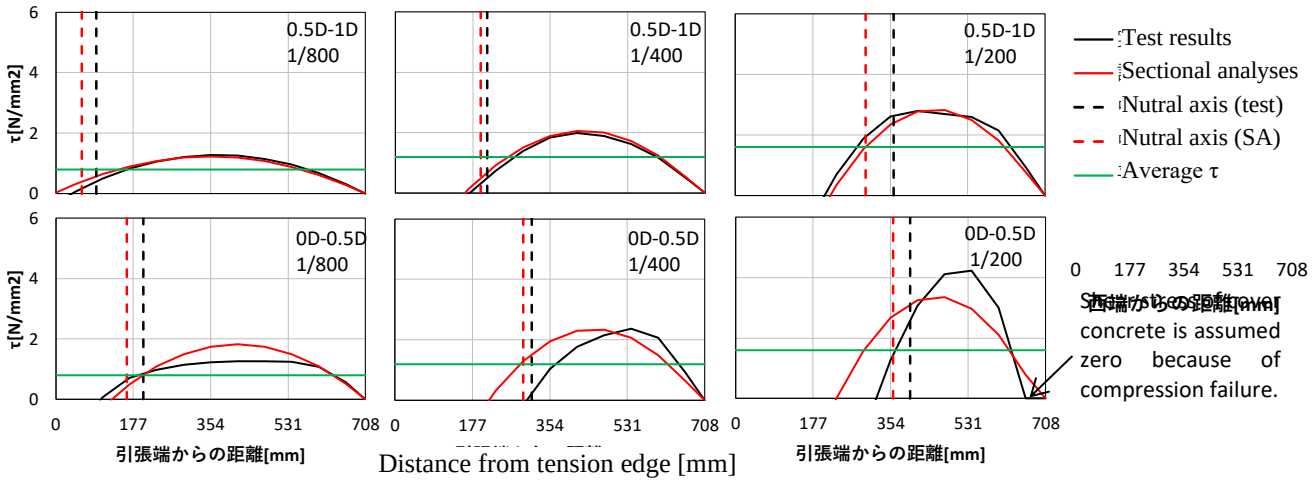

Fig.10 Shear stress distribution in horizontal section

3.2 Shear displacement

Shear displacement is obtained by subtracting flexural displacement from the total displacement and shown in Fig. 11. In the figure, elastic shear displacement that is obtained by Eq.(4) is also shown by red dashed line.

$$\delta_s = \int \frac{Q}{GA_e(z)} dz \tag{4}$$

where Q [kN] is the shear force, G [kN/mm^2] is the shear modulus of the concrete, and $A_e(z)$[mm^2] is the sectional area at height z [m] that excludes area of flexural cracks and compression failure. Gray line shows the test results computed using the flexural displacement obtained based on the vertical displacement gauges attached to the side of the specimen [7]. From the figure, test results obtained using motion capture data (black solid line) well corresponds to the effective elastic shear displacement (red dashed line). It shows no shear

crack was caused until 1/133 rad. The shear displacement is smaller than 10 % of the flexural displacement (Fig.8). On the contrary, test results based on the vertical displacement gauges (gray line) is found overestimated. This is because flexural displacement, which is subtracted from the total displacement in computing shear displacement, is underestimated by using average rotation angle of whole section that is lower than that of compression side (see Fig. 6).

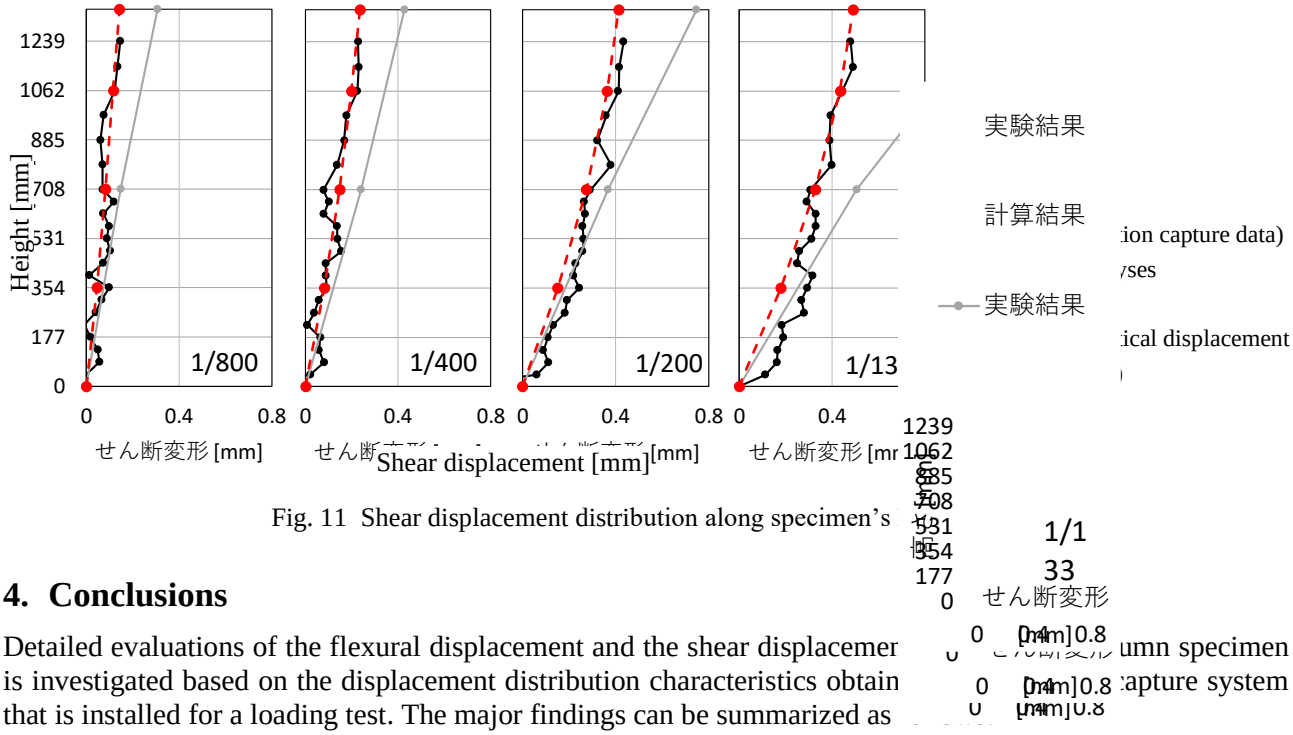

Fig. 11 Shear displacement distribution along specimen's

4. Conclusions

Detailed evaluations of the flexural displacement and the shear displacemer umn specimen is investigated based on the displacement distribution characteristics obtain apture system that is installed for a loading test. The major findings can be summarized as

1. Rotation angle of the tension side concrete is smaller than that of the compression side concrete because cantilever portion between two flexural cracks in the tension side is pulled down by the downward force due to the flexural rebars. Displacement of the compression side is focused on in the discussion of the horizontal displacement of the column specimen as a component of a structural frame.
2. The flexural displacement calculated based on the sectional analyses is underestimated compared to the test results that is computed by integrating rotation angle of the compression side (about 30 % at 1/200 rad.). If it is modified considering the larger curvature of the test results at the bottom section, calculation well evaluate the test results. The larger curvature of the test results in the compression side is assumed to be caused by the restraint effect by the stub (footing or beam in the actual structures) that increase the shear stress, accordingly, increase curvature in the compression side.
3. Shear displacement obtained by subtracting flexural displacement from the total displacement can be well evaluated by the elastic shear displacement considering sectional area that excludes area of crack and compression failure.

The effect of stub restraint on the flexural displacement should be evaluated quantitatively for the highly accurate evaluation of the column displacement.

5. Acknowledgements

A part of this research is carried out as a project to promote building standards development in the Ministry of Land, Infrastructure, Transport and Tourism in FY2018.

6. References

[1] National Institute for Land and Infrastructure Management/ Building Research Institute (2015): Commentary on provisions in building standard law concerning structures of buildings.

[2] Sugano, S. (1973): Research on load – displacement characteristics of reinforced concrete members, *Concrete Journal*, Vol. 11, issue 2, pp.1-9.

[3] Architectural Institute in Japan (2010): *AIJ Standard for Structural Calculation of Reinforced Concrete Structures* .

[4] Architectural Institute in Japan (2004): *Guidelines for Performance Evaluation of Earthquake Resistant Reinforced Concrete Buildings (Draft)*.

[5] Jeong, M., Maeda, M., Kimura, S., Kabeyazawa, T., Yukimura, N., and Osada, M. (1999): Behavior of Reinforced Concrete Beams under Axial Restriction - Part 4 Evaluation of Yielding Deformation, *Summaries of technical papers of AIJ annual meeting*, pp. 891-892.

[6] Priestley, M., Calvi, G. and Kowalski, M. (2007): *Displacement-based seismic design of structures*. IUSS Press, Pavia.

[7] Asai, T., Teshigawara, M. (2019): “Study on more accurate evaluation of yielding displacement of RC column”, *Proceedings of the Japan Concrete Institute*, 2019, Vol.41, No. 2, pp.139-144. (in Japanese)

[8] Teshigawara, M., Asai, T. et al.: A study on Damping Property of RC Structures – Part 1 – 6, *Summaries of technical papers of AIJ annual meeting*, pp.623-638

